Spleen Tyrosine Kinase Contributes to Müller Glial Expression of Proangiogenic Cytokines in Diabetes

Esma I. Yerlikaya,[1] Allyson L. Toro,[1] Siddharth Sunilkumar,[1] Ashley M. VanCleave,[1] Ming Leung,[2] Yuka Imamura Kawasawa,[2] Scot R. Kimball,[1] and Michael D. Dennis[1,3]

[1]Department of Cellular and Molecular Physiology, Penn State College of Medicine, Hershey, Pennsylvania, United States
[2]Department of Pharmacology, Penn State College of Medicine, Hershey, Pennsylvania, United States
[3]Department of Ophthalmology, Penn State College of Medicine, Hershey, Pennsylvania, United States

Correspondence: Michael D. Dennis, Department of Cellular and Molecular Physiology, H166, Penn State College of Medicine, 500 University Drive, Hershey, PA 17033, USA; mdennis@psu.edu.

Received: July 7, 2022
Accepted: October 2, 2022
Published: October 28, 2022

Citation: Yerlikaya EI, Toro AL, Sunilkumar S, et al. Spleen tyrosine kinase contributes to Müller glial expression of proangiogenic cytokines in diabetes. *Invest Ophthalmol Vis Sci.* 2022;63(11):25. https://doi.org/10.1167/iovs.63.11.25

Purpose. Neuroglial dysfunction occurs early in the progression of diabetic retinopathy. In response to diabetes or hypoxia, Müller glia secrete cytokines and growth factors that contribute to disease progression. This study was designed to examine common signaling pathways activated in Müller glia by both type 1 and pre-/type 2 diabetes.

Methods. RiboTag (*Pdgfra*-cre;HA-Rpl22) mice were used to compare the impact of streptozotocin (STZ) and a high-fat, high-sucrose (HFHS) diet on ribosome association of mRNAs in Müller glia by RNA sequencing analysis. Human MIO-M1 Müller cells were exposed to either hyperglycemic or hypoxic culture conditions. Genetic manipulation and pharmacologic inhibition were used to interrogate signaling pathways.

Results. Association of mRNAs encoding triggering receptor expressed on myeloid cells 2 (TREM2), DNAX-activating protein 12 kDa (DAP12), and colony stimulating factor 1 receptor (CSF1R) with ribosomes isolated from Müller glia was upregulated in both STZ diabetic mice and mice fed an HFHS diet. The TREM2/DAP12 receptor-adaptor complex signals in coordination with CSF1R to activate spleen tyrosine kinase (SYK). SYK activation was enhanced in the retina of diabetic mice and in human MIO-M1 Müller cell cultures exposed to hyperglycemic or hypoxic culture conditions. DAP12 knockdown reduced SYK autophosphorylation in Müller cells exposed to hyperglycemic or hypoxic conditions. SYK inhibition or DAP12 knockdown suppressed hypoxia-induced expression of the transcription factor hypoxia-inducible factor 1α (HIF1α), as well as expression of vascular endothelial growth factor and angiopoietin-like 4.

Conclusions. The findings support TREM2/DAP12 receptor-adaptor complex signaling via SYK to promote HIF1α stabilization and increased angiogenic cytokine production by Müller glia.

Keywords: diabetic retinopathy, mRNA translation, glia, hyperglycemia, hypoxia

Despite recent advances in treatment through blockade of vascular endothelial growth factor (VEGF), diabetic retinopathy (DR) remains one of the most frequent causes of new cases of blindness. The incidence of pre- and type 2 diabetes is rapidly on the rise and accounts for most DR prevalence. The etiology and management of patients with type 1 and type 2 diabetes differ. Type 1 diabetes is defined by an absolute deficiency of insulin secretion, whereas type 2 diabetes involves a progression of overnutrition, hyperinsulinemia, insulin resistance, and an inadequate compensatory insulin secretory response. Moreover, pre- and type 2 diabetes often involve hyperlipidemia, which is independently associated with the development of DR.[1] At present, understanding of common molecular events in type 1 and type 2 diabetes that contribute to early retinal dysfunction is limited.

DR in both type 1 and type 2 diabetes is ultimately defined by clinically visible microvascular abnormalities; however, loss of neurovascular coupling, neurodegeneration, gliosis, and neuroinflammation occur before the development of clinically visible microvascular pathologies.[2] Activation of retinal glia likely serves as an adaptive response to mitigate damage to retinal neurons and vasculature. Müller glia are the principal glia of the retina and provide critical homeostatic, metabolic, and structural support that links all other elements of the retina, including photoreceptors, neurons, and vasculature.[3] In response to diabetes, prolonged changes in the expression of Müller glia-derived factors contribute to the development of vascular defects and neuronal dysfunction.[4] In fact, deletion of VEGF specifically in Müller glia is sufficient to prevent elevated retinal VEGF protein expression and reduce retinal vascular pathology in diabetic mice.[5]

VEGF expression is classically regulated by the master transcription factor hypoxia-inducible factor 1 (HIF1).[6] VEGF transactivation is mediated by multiple hypoxia response elements (HREs) in the VEGF mRNA 5′- and 3′-untranslated region (UTR) sequences. HIF1 is a heterodimer

Copyright 2022 The Authors

This work is licensed under a Creative Commons Attribution-NonCommercial-NoDerivatives 4.0 International License.

Investigative Ophthalmology & Visual Science

composed of HIF1α and HIF1β. HIF1 activity is principally regulated through variation in HIF1α protein half-life.[7] Under normoxic conditions, HIF1α is hydroxylated at P402/P564 by prolyl hydroxylase domain (PHD) enzymes, leading to its ubiquitination and rapid degradation by the proteasome. In response to hypoxia, PHD activity is impaired, resulting in HIF1α accumulation. Cytoplasmic HIF1α enters the nucleus to form a complex with the constitutively expressed HIF1β subunit and bind to the HREs of an array of proangiogenic target genes. HIF1α mRNA expression is observed throughout the human retina but is most highly expressed in Müller glia.[8] Indeed, HIF1α protein localizes to Müller glia in the retina of patients with diabetic eye disease.[9]

The studies here were designed to identify common signaling pathways activated in retinal Müller glia by both type 1 (i.e., streptozotocin [STZ]–induced diabetes) and pre-/type 2 diabetes (i.e., prodiabetogenic diet). Both of these preclinical murine models develop retinal pathology characterized by gliosis, neurodegeneration, and vascular injury.[10,11] Sequencing analysis of ribosome-associated mRNAs from retinal Müller glia revealed a common increase in mRNAs encoding triggering receptor expressed on myeloid cells 2 (TREM2), DNAX-activating protein of 12 kDa (DAP12, also known as *Tyrobp*), and colony stimulating factor 1 receptor (CSF1R). Recent studies support a role for TREM2/DAP12 activation in the transformation of microglia from a homeostatic to a neural disease-associated state,[12] but a role for this receptor-adaptor complex in Müller glia has not been previously reported. TREM2/DAP12 signals in coordination with CSF1R to promote activation of spleen tyrosine kinase (SYK).[13] SYK inhibition in STZ diabetic rats was recently found to reduce retinal vascular permeability, prevent the appearance of acellular capillaries, and restore expression of tight junction proteins.[14] Importantly, the benefits of SYK inhibition were attributed, at least in part, to normalization of VEGF expression in the retina of STZ diabetic rats. A role for SYK in regulation of HIF1 has been previously demonstrated in splenocytes and macrophages.[15,16] Thus, the studies here investigated a role for TREM2/DAP12 signaling via SYK to facilitate upregulation of HIF1α and increased cytokine expression by Müller glia.

Materials and Methods

Animals

Pdgfra-cre;HA-Rpl22 (RiboTag) mice were generated as previously described.[17] Male littermates were administered 50 mg/kg STZ versus sodium citrate buffer for 5 consecutive days or fed a high-fat, high-sucrose diet (HFHS, ENVIGO TD.88137; Envigo, Indianapolis, IN, USA) versus control chow (ENVIGO TD.08485) to induce diabetes. Diabetic phenotype was assessed with fasting blood glucose levels >250 mg/dL. All procedures were approved by the Penn State College of Medicine Institutional Animal Care and Use Committee and were in accordance with the ARVO statement for the ethical use of animals in ophthalmic and vision research.

Immunofluorescent Microscopy

Immunofluorescent microscopy was performed as previously described.[18] Whole eyes were extracted, placed in 4% paraformaldehyde for 30 minutes, and then washed with PBS. After 48 hours of incubation in 30% sucrose at 4°C, the eyes were placed in optimal cutting temperature compound, flash-frozen, and sectioned. Retinal cryosections (10 µm) were permeabilized with 0.1% Triton-X-100 in PBS, blocked with 10% donkey serum, and incubated in anti–glutamine synthetase (GS) primary antibody followed by Alexa Fluor 488 secondary antibody (Supplementary Table S1). Sections were blocked and incubated in anti-hemagglutinin (HA) primary antibody and Alexa Fluor 647 secondary antibody. Hoechst (1.6 mmol/L) was used for nuclear staining in all sections. Imaging was performed with a Leica SP8 confocal laser microscope (Leica Biosystems, Wetzlar, Germany).

Ribosome-Associated RNA Isolation

Retinas from three mice per group were extracted from Ribotag mice, and HA-tagged ribosomes were immunoprecipitated as previously described.[17] Anti-HA beads (EZview; Sigma, St. Louis, MO, USA) were washed and blocked in 0.5% BSA. Retinas were homogenized in polysome buffer and centrifugated at 10,000 × *g* at 4°C for 10 minutes. Supernatants were collected and combined with beads at 4°C for 16 hours. The mixture was centrifugated at 8200 × *g* for 30 seconds, the pellet was collected, and the beads were washed with high-salt buffer. RLT buffer (Qiagen, Hilden, Germany) was added to beads for processing, and RNA was isolated using the RNeasy Micro kit (Qiagen).

Sequencing Analysis

TruSeq Stranded mRNA Library Prep kit (Illumina, San Diego, CA, USA) was used to prepare cDNA libraries as per the manufacturer's instructions. Briefly, polyA RNA was purified from 200 ng total RNA using oligo (dT) beads. The extracted mRNA fraction was subjected to fragmentation, reverse transcription, end repair, 3′-end adenylation, and adaptor ligation, followed by PCR amplification and SPRI bead purification (Beckman Coulter, Pasadena, CA, USA). Unique dual index sequences (NEXTFLEX Unique Dual Index Barcodes; BioO Scientific, Austin, TX, USA) were incorporated in the adaptors for multiplexed high-throughput sequencing. The final product was assessed for its size distribution and concentration using the BioAnalyzer High Sensitivity DNA Kit (Agilent Technologies, Santa Clara, CA). Libraries were pooled and diluted to 3 nM with 10 mM Tris-HCl, pH 8.5, and then denatured using the Illumina protocol. The denatured libraries were loaded onto an S1 flow cell on an Illumina NovaSeq 6000 (Illumina) and run for 2 × 50 cycles according to the manufacturer's instructions. De-multiplexed and adapter-trimmed sequencing reads were generated using Illumina bcl2fastq (released version 2.20.0.422), allowing no mismatches in the index read. BBtools (ver. 36.49) was used to trim/filter low-quality sequences using the "qtrim=lr trimq=10 maq=10" option. Reads were then mapped to reference mouse genome mm10 using hisat2 (ver. 2.1.0) with –no-mixed and –no-discordant options. Read counts were calculated using HTSeq (ver. 0.11.2) by supplementing Ensembl gene annotation (Mus_musculus.GRCm38.78_ERCC92.gtf). Differential analysis was performed using edgeR exactTest, with the biological coefficient of variation manually set to 0.1. Ingenuity Pathway Analysis software was used to preform gene ontology analysis on the significant genes identified by the differential analysis.

Investigative Ophthalmology & Visual Science

Cell Culture

Human MIO-M1 Müller cells were obtained from the UCL Institute of Ophthalmology (London, UK) and cultured at 37°C and 5% CO_2 in Dulbecco's modified eagle medium (DMEM) containing 1 g/L glucose with 10% heat-inactivated fetal bovine serum (FBS) and 1% penicillin-streptomycin (P/S). Culture medium was supplemented with 25 mM D-glucose (BioChemika, Steinheim, Germany) to model hyperglycemic conditions. For hypoxic conditions, cells were cultured in a hypoxia chamber (Hypoxia Incubator Chamber Cat# 27310; STEMCELL Technologies, Vancouver, Canada) containing mixed gas (1% O_2, 94% N_2, and 5% CO_2). In some studies, culture medium was supplemented with $CoCl_2$ (150 µM), deferoxamine mesylate (DFO, 100 µM), or carbobenzoxy-Leu-Leu-leucinal (MG132, 20 µM). ER-2739 maleate (30 µM) (Tocris Bioscience, Bristol, United Kingdom) or fostamatinib disodium (R788, 10 µM) (MedChemExpress, Princeton, NJ, USA) was added to culture medium 15 minutes prior to other manipulations. HEK293 cells were cultured in high-glucose (4.5 g/L) DMEM, 10% FBS, and 1% P/S. HEK293 cells were transfected with plasmids encoding empty vector, HIF1α wild-type, or HIF1α P402A/P564A using Lipofectamine 2000 (Thermo Fisher Scientific, Waltham, MA, USA). HA-HIF1α-pcDNA3 and HA-HIF1α P402A/P564A-pcDNA3 were a gift from William Kaelin (Addgene plasmids #18949 & 18955). pLKO-shDAP12 plasmid for lentiviral short hairpin RNA (shRNA) knockdown was obtained from the Penn State College of Medicine shRNA Library Core. pLKO.1-TRC control shRNA plasmid was a gift from David Root (Addgene plasmid #10879). HEK293FT cells were used to generate lentivirus containing either the control shRNA or an shRNA targeting DAP12 (5′-CCGGCCTCTCCTGCTGGCTGTAAGTCTCGAG ACTTACAGCCAGCAGGAGAGGTTTTTG-3′). Lentivirus was applied to MIO-M1 cells to obtain cell lines with stable shRNA expression as previously described.[19]

Western Blotting

Cells were lysed, combined with Laemmli sample buffer, and boiled at 100°C for 5 minutes. Then, 4% to 20% Criterion gels (Bio-Rad, Hercules, CA, USA) were used for SDS-PAGE. Proteins were transferred to nitrocellulose (Thermo Scientific) or polyvinylidene fluoride (PVDF) membrane (Bio-Rad), which was blocked with 5% milk in TBST (50 mM Tris, pH 7.6; 0.9% NaCl; and 0.1% Tween-20) and exposed to the appropriate primary and secondary antibody (Supplementary Table S1). Protein bands were visualized with enhanced chemiluminescence Clarity Reagent (Bio-Rad) using a ProteinSimple FluorChem E.

Quantitative RT-PCR

Cells were collected with TRIzol for homogenization, and RNA was extracted following the organic-extraction protocol (Invitrogen, Carlsbad, CA, USA). Whole murine retinas were homogenized in TRIzol, combined with chloroform, and centrifuged to separate the organic and aqueous phases. The aqueous phase was collected and RNA was isolated using an RNeasy micro kit (Qiagen). A High-Capacity cDNA Reverse Transcription Kit (Thermo Fisher Scientific) was used to generate cDNA. Quantitative RT-PCR was conducted using a QuantiTect SYBR Green PCR Kit (Qiagen). Primer sequences are listed in Supplementary Table S2. Results were normalized to GAPDH using the $2^{-\Delta\Delta CT}$ calculations.

Data Analysis and Presentation

Statistical analyses were performed using GraphPad Prism software (GraphPad Software, La Jolla, CA, USA) with $P < 0.05$ defined as statistically significant. Data were analyzed overall with either Student's *t*-test or one-way or two-way analysis of variance. Trend test and pairwise comparisons were conducted with the Tukey test for multiple comparisons. Figures were assembled with Adobe Illustrator (Adobe, San Jose, CA, USA). Graphics were created with BioRender.com.

Results

Examination of mRNA Translation in Retinal Müller Glia

To specifically assess ribosome-associated mRNAs in retinal Müller glia, a previously developed RiboTag mouse that expresses an epitope-tagged variant of the ribosomal protein Rpl22 under the control of Cre recombinase was used.[20] In Cre-positive cells, wild-type exon 4 of Rpl22 was replaced with an HA-tagged exon 4 (Fig. 1A). $Rpl22^{HA}$ expression was directed to Müller glia under the control of *Pdgfra*-cre recombinase.[21] Specificity of $Rpl22^{HA}$ expression in Müller glia of $Rpl22^{HA}$; *Pdgfra*-cre mice[17] was assessed by examining retinal cross sections. Consistent with the prior analysis,[17] $Rpl22^{HA}$ was observed in radially oriented processes that spanned the entire neuroretina and in branching end feet that surrounded ganglion cells (Fig. 1B). $Rpl22^{HA}$ strongly colocalized with the Müller glia marker GS. $Rpl22^{HA}$ forms a fully functional 60S ribosomal subunit that allowed translationally active mRNAs from Pdgfra-cre expressing Müller glia to be isolated from whole retina tissue homogenate by affinity purification (Fig. 1C). To evaluate the impact of type 1 diabetes on Müller glial mRNA translation, mice were administered STZ. After 6 weeks of STZ-induced diabetes, mice exhibited increased fasting blood glucose concentrations (Fig. 1D). To evaluate the impact of type 2 diabetes, mice were fed an HFHS diet. After 6 weeks of the prodiabetogenic diet, fasting blood glucose concentrations were elevated (Fig. 1E) and weight gain increased (Fig. 1F), resulting in greater body weight (Fig. 1G). RNA sequencing was performed on mRNAs associated with $Rpl22^{HA}$ ribosomes in the retina of STZ diabetic versus nondiabetic control mice (Fig. 1H, Supplementary Table S3). Most transcripts observed in the analysis of STZ versus vehicle control did not exhibit a change in abundance ($R^2 = 0.999$). A similar sequencing analysis was also performed on $Rpl22^{HA}$-associated mRNAs from the retina of mice fed either an HFHS diet or control chow ($R^2 = 0.995$, Fig. 1I, Supplementary Table S4). Whereas the abundance of $Rpl22^{HA}$ ribosome-associated mRNAs was highly similar in nondiabetic control versus chow-fed mice ($R^2 = 0.999$, Fig. 1J), increased variation was observed in the abundance of $Rpl22^{HA}$ ribosome-associated mRNAs from the retina of STZ diabetic versus HFHS diet-fed mice ($R^2 = 0.994$, Fig. 1K). The analysis supports variation in ribosome-association of mRNAs within each preclinical model of diabetes and substantial variation between the two experimental models.

Upregulation of Müller Glial Trem2/DAP12 Signaling in Diabetes

STZ diabetes enhanced the abundance of 28 mRNAs in the $Rpl22^{HA}$ ribosome immunoprecipitate and reduced the

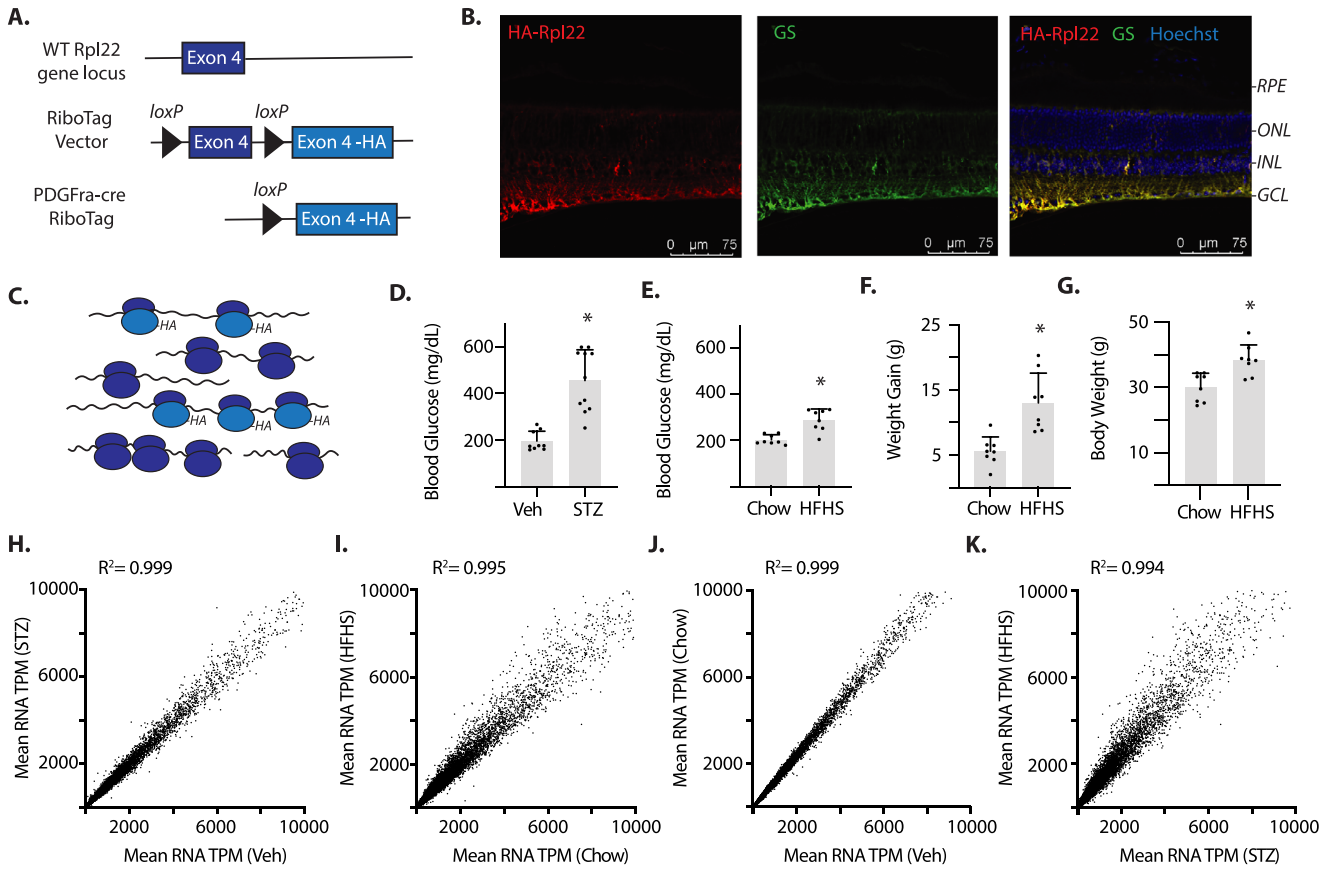

Figure 1. Ribosome-associated mRNAs isolated from retinal Müller glia of diabetic mice were examined by sequencing analysis. (**A**) Müller glia-specific expression of HA-tagged Rpl22 protein was achieved by Cre-Lox recombination, resulting in deletion of the wild-type (WT) exon 4 of Rpl22 and replacement with an HA-tagged Rpl22 exon in the presence of *Pdgfra*-cre. (**B**) Whole eyes were isolated, fixed, and sectioned longitudinally. Localization of HA-Rpl22 (*red*) and the Müller glia marker GS (*green*) was evaluated by immunofluorescence. Nuclei were visualized with Hoechst (*blue*). (**C**) Ribosomes from Müller glia of Rpl22^{HA}-expressing homozygous mouse retinas were isolated by immunoprecipitation. Cell-specific expression of Rpl22^{HA} allows translationally active mRNAs from Müller glia to be isolated from whole retina tissue homogenate by affinity purification, as all cre-negative cells express wild-type Rpl22 that lacks an affinity tag. (**D**) Diabetes was induced in Rpl22^{HA} mice by administration of STZ. Control mice received a vehicle (Veh). Fasting blood glucose concentrations were measured after 6 weeks. (**E–G**) Mice were fed either an HFHS diet or control chow for 6 weeks. Fasting blood glucose concentrations were measured (**E**). Weight gain (**F**) and final body weight (**G**) were determined. (**H**) Retinas were analyzed after 6 weeks of STZ diabetes. Rpl22^{HA} ribosome-associated mRNAs were evaluated by RNA sequencing. Variation in Rpl22^{HA} ribosome-associated mRNA abundances in mice receiving STZ or Veh was visualized. (**I**) Retinas were analyzed 6 weeks after initiation of HFHS or chow diet. Changes in Rpl22^{HA} ribosome-associated mRNAs in mice receiving the HFHS diet or chow were compared. (**J**) Rpl22^{HA} ribosome-associated mRNA sequencing analysis for control mice receiving either Veh or chow diet was compared. (**K**) Rpl22^{HA} ribosome-associated mRNAs from Müller glia of mice receiving either STZ or HFHS diet were compared. Values are means ± SD. *$P < 0.05$ versus Veh or chow. GCL, ganglion cell layer; INL, inner nuclear layer; ONL, outer nuclear layer; RPE, retinal pigment epithelium; TPM, transcript per million.

abundance of 48 mRNAs, as compared to nondiabetic control mice (Fig. 2A). Rpl22^{HA} ribosome association was increased for 58 mRNAs in the retina of mice fed an HFHS as compared to control chow, and 61 mRNAs were decreased (Fig. 2B). To assess the potential impact of the observed changes, functional relationships between mRNAs that exhibited altered ribosome association were investigated. The top canonical pathways identified by Ingenuity Pathway Analysis as being altered by STZ diabetes included Interferon Signaling and the GP6 Signaling Pathway (Supplementary Fig. S1). The top scoring pathways identified as being altered by the HFHS diet included Regulation of Epithelial-Mesenchymal Transition Pathway and IL-4 Signaling (Supplementary Fig. S2).

Surprisingly, there was limited overlap in the mRNAs that were altered in both mouse models, as only 18 mRNAs exhibited codirectional changes (Figs. 2C, 2D). Nineteen mRNAs were upregulated with the HFHS diet but downregulated with STZ diabetes. The opposite case, in which an mRNA was upregulated with STZ diabetes but downregulated by the HFHS diet, was not observed. Notably, mRNAs encoding all three subunits of the complement protein C1q were upregulated in both models (Fig. 2D), and codirectional changes were observed for several mRNAs encoding crystallins. Additionally, mRNAs encoding DAP12, TREM2, and CSF1R all exhibited enhanced association with Rpl22^{HA} ribosomes in both STZ diabetic mice and mice fed an HFHS diet. TREM2 and CSF1R are cell receptors that cross-talk to drive glial activation (Fig. 2E). DAP12 binds the intracellular domain of TREM2, and CSF1R cross-talks with TREM2/DAP12 by promoting Src-dependent phosphorylation of DAP12.[22] In contrast with the sequencing

Investigative Ophthalmology & Visual Science

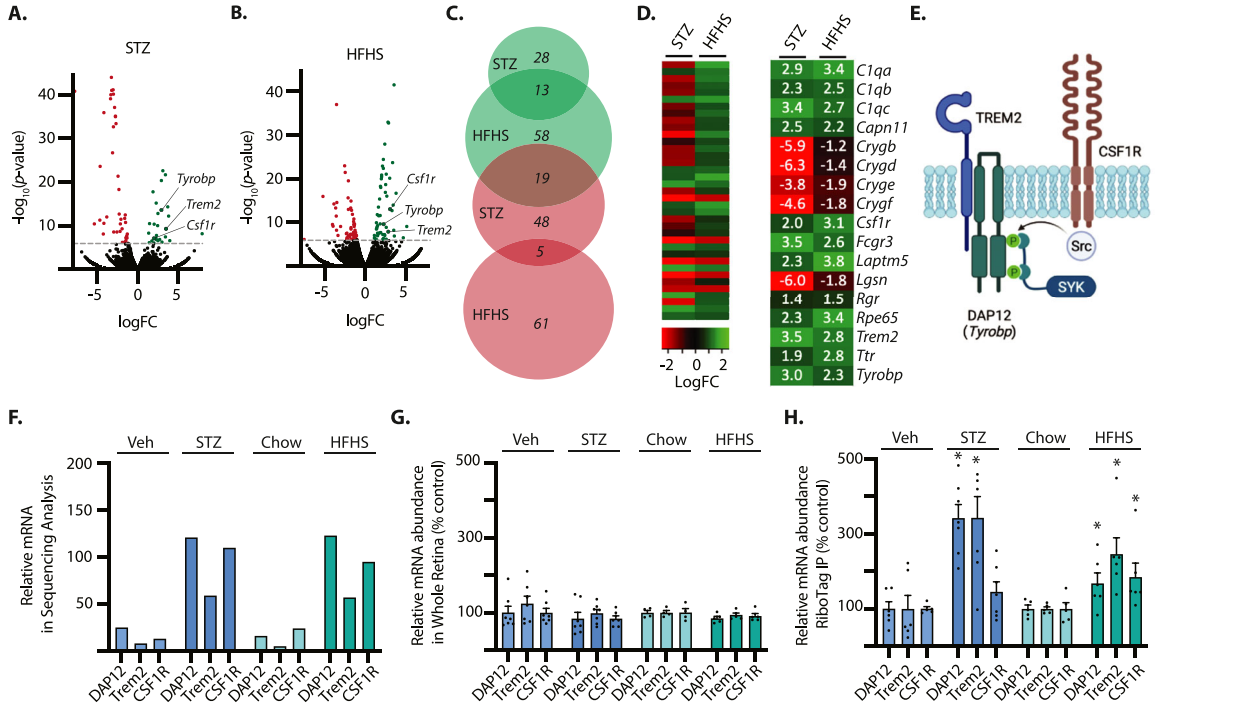

Figure 2. Ribosome association of mRNAs encoding proteins in the TREM2/DAP12 signaling pathway was increased in Müller glia of diabetic mice. Diabetes was induced in Rpl22^{HA} mice by administration of STZ. Control mice received a vehicle (Veh). Retinas were analyzed after 6 weeks of diabetes. Ribosomes from Müller glia of Rpl22^{HA}-expressing homozygous mice were isolated from retina homogenates by immunoprecipitation (IP) and examined by RNA sequencing. Mice were fed either an HFHS diet or control chow. Retinas were analyzed 6 weeks after initiation of diet. (**A**, **B**) Volcano plot of sequencing analysis for STZ diabetic versus Veh control mice (**A**) and HFHS diet versus chow (**B**) with mRNAs exhibiting increased (*green*) or decreased (*red*) Rpl22^{HA} association shown. (**C**) Overlap in mRNAs exhibiting changes in Rpl22^{HA} association in mice receiving STZ versus Veh or HFHS diet versus chow was visualized by Venn diagram. (**D**) Heatmap (*left*) illustrates mRNAs exhibiting changes in ribosome association in both models. Expanded view of heatmap (*right*) depicts only the mRNAs exhibiting codirectional changes in the two models, with log fold change (FC) value shown in *white*. (**E**) Cartoon of TREM2/DAP12 signaling to activate Syk kinase is shown. (**F**) Results from the sequencing analysis for DAP12 (*Tyrobp*), TREM2, and CSF1R. (**G**) DAP12, TREM2, and CSF1R mRNA abundance was examined in whole retinal lysates by quantitative PCR (qPCR). (H) Ribosome-associated mRNAs from Müller glia were isolated by immunoprecipitation. DAP12, TREM2, and CSF1R mRNA abundance was examined in retinal immunoprecipitate by qPCR. Values are means ± SD. *$P < 0.05$ versus Veh or chow.

analysis of Rpl22^{HA} ribosome-associated mRNAs (Fig. 2F), DAP12, TREM2, and CSF1R mRNA abundance in homogenates from whole retina was not altered with either STZ diabetes or the HFHS diet (Fig. 2G). In support of the sequencing data, PCR analysis confirmed increased DAP12 and TREM2 association with Rpl22^{HA} ribosomes from the retina of STZ diabetic mice or mice fed an HFHS diet (Fig. 2H). Increased CSF1R association with Rpl22^{HA} ribosomes was also observed in mice fed an HFHS diet, and there was a trend toward upregulation in STZ diabetic mice ($P = 0.0937$).

SYK Activation was Enhanced in the Retina of Diabetic Mice

To further explore TREM2/DAP12 signaling, we investigated SYK activation by assessing autophosphorylation of the kinase. SYK autophosphorylation within its activation loop at Tyr525/Tyr526 is required for SYK downstream signaling.[23] SYK phosphorylation was enhanced in retinal lysates from STZ diabetic mice as compared to nondiabetic controls (Fig. 3A). Enhanced SYK phosphorylation was also observed in mice fed an HFHS diet as compared to a chow diet (Fig. 3B). Together, the data provide direct evidence of enhanced SYK activation in the retina of diabetic mice.

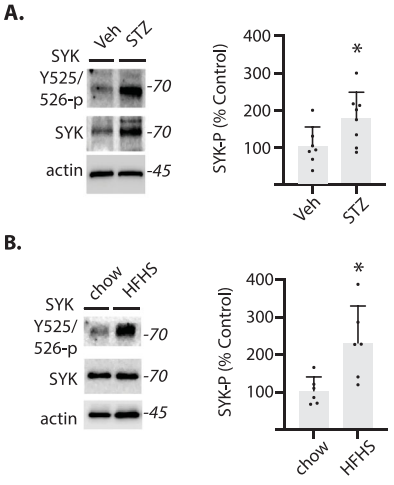

Figure 3. SYK autophosphorylation was enhanced in the retina of diabetic mice. (**A**) Phosphorylation of SYK at Tyr525/Tyr526 was evaluated in retinal lysates from mice administered either STZ or vehicle (Veh) by Western blotting. Representative blots are shown. Protein molecular mass in kDa is indicated at *right* of blots. (**B**) SYK phosphorylation was evaluated in retinal lysates from mice fed either an HFHS diet or control chow. Values are means ± SD. *$P < 0.05$ versus Veh or chow.

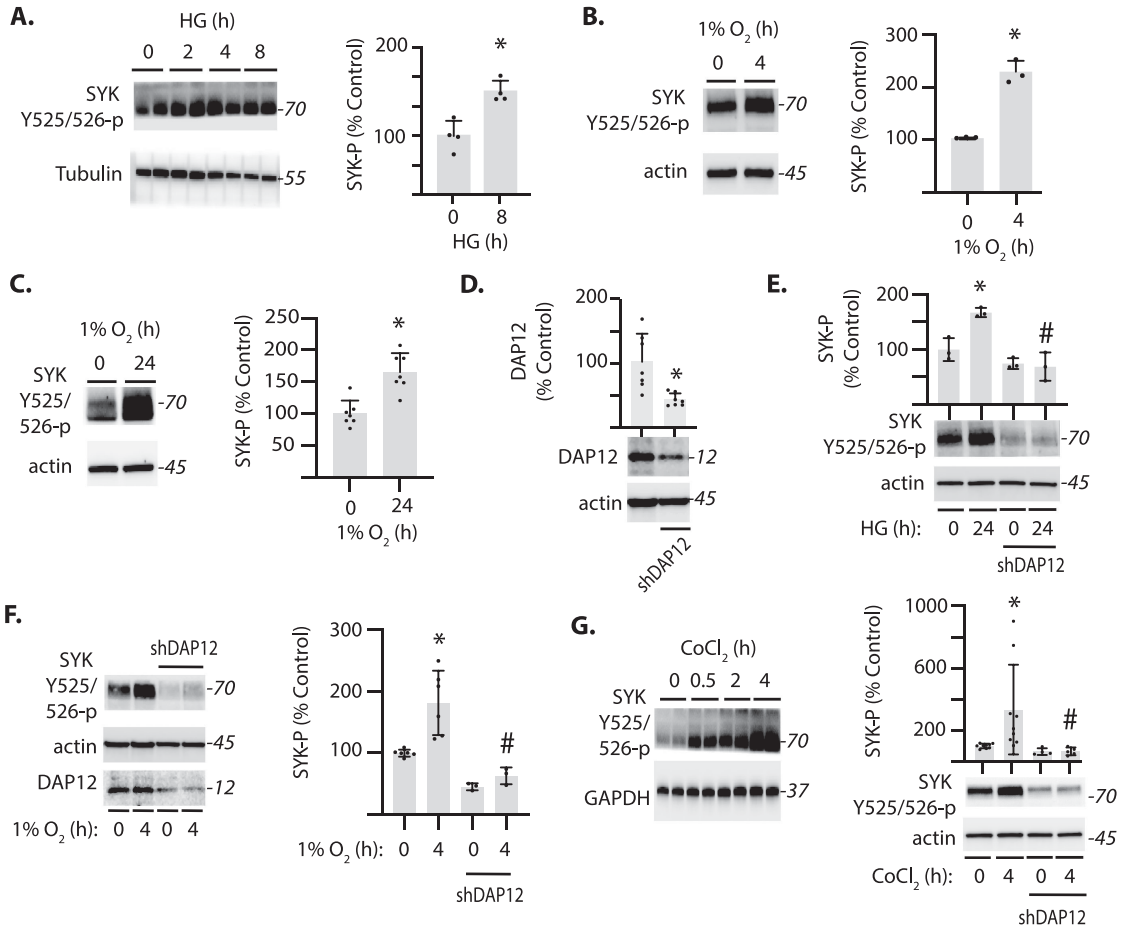

Figure 4. Phosphorylated SYK was enhanced in Müller cells by hyperglycemic or hypoxic conditions. (**A**) MIO-M1 Müller cells were exposed to medium containing 30 mM glucose (high glucose, HG) for up to 8 hours. SYK phosphorylation at Tyr525/Tyr526 was evaluated by Western blotting. Representative blots are shown. Protein molecular mass in kDa is indicated at *right* of blots. Phosphorylated SYK was quantified after 8 hours of exposure to HG. (**B**, **C**) SYK phosphorylation was evaluated in MIO-M1 cells exposed to hypoxic conditions for 4 (**B**) or 24 (**C**) hours. (**D**) DAP12 expression was knocked down in MIO-M1 cells by stable expression of an shRNA (shDAP12). (**E**) MIO-M1 cells were exposed to HG for 24 hours and SYK phosphorylation was quantified. (**F**) MIO-M1 cells were exposed to 1% oxygen for 4 hours and SYK phosphorylation was quantified. (**G**) MIO-M1 cells were exposed to medium supplemented with $CoCl_2$ for up to 4 hours. SYK phosphorylation was quantified after 0 or 4 hours of exposure to $CoCl_2$ (**G**). Values are means ± SD. $^*P < 0.05$ versus time 0; $^\#P < 0.05$ versus without shDAP12.

DAP12 Contributes to Enhanced SYK Activation in Müller Glia

To investigate SYK activation in human Müller glia, SYK phosphorylation was examined in immortalized MIO-M1 Müller cell cultures. Phosphorylated SYK was increased in cells exposed to either hyperglycemic (Fig. 4A) or hypoxic culture conditions (Figs. 4B, 4C). To evaluate a role for TREM2/DAP12 signaling in SYK activation, DAP12 was knocked down by stable expression of an shRNA (Fig. 4D). DAP12 knockdown prevented an increase in phosphorylated SYK in cells exposed to either hyperglycemic (Fig. 4E) or hypoxic culture conditions (Fig. 4F, Supplementary Fig. S3A). Upregulation of phosphorylated SYK was also observed upon exposure to the hypoxia-mimetic $CoCl_2$ (Fig. 4G), in coordination with the gliosis marker GFAP (Supplementary Fig. S3B). DAP12 knockdown also prevented an increase in phosphorylated SYK with $CoCl_2$ exposure (Fig. 4G).

SYK Inhibition Suppressed HIF1α Expression Under Hypoxic Conditions

To investigate the consequence of hypoxia-induced TREM2/DAP12 signaling via SYK, HIF1α expression was examined in Müller cell cultures exposed to hypoxic conditions. Hypoxia promoted HIF1α expression in MIO-M1 cells (Supplementary Fig. S3C), and the effect was blunted by DAP12 knockdown (Fig. 5A, Supplementary Fig. S3D). Hypoxia prevents proteasomal degradation of HIF1α by suppressing PHD activity, which is modeled by $CoCl_2$- and DFO-induced PHD inhibition. HIF1α expression was increased in MIO-M1 cells exposed to $CoCl_2$, and DAP12 knockdown attenuated the effect (Fig. 5B). In support of a role for SYK signaling in promoting HIF1α expression, SYK inhibition with ER-27391 prevented the increase in HIF1α expression with either hypoxia (Fig. 5C) or $CoCl_2$ (Fig. 5D). SYK inhibition also prevented an increase in HIF1α expression in cells exposed to the iron chelator

Investigative Ophthalmology & Visual Science

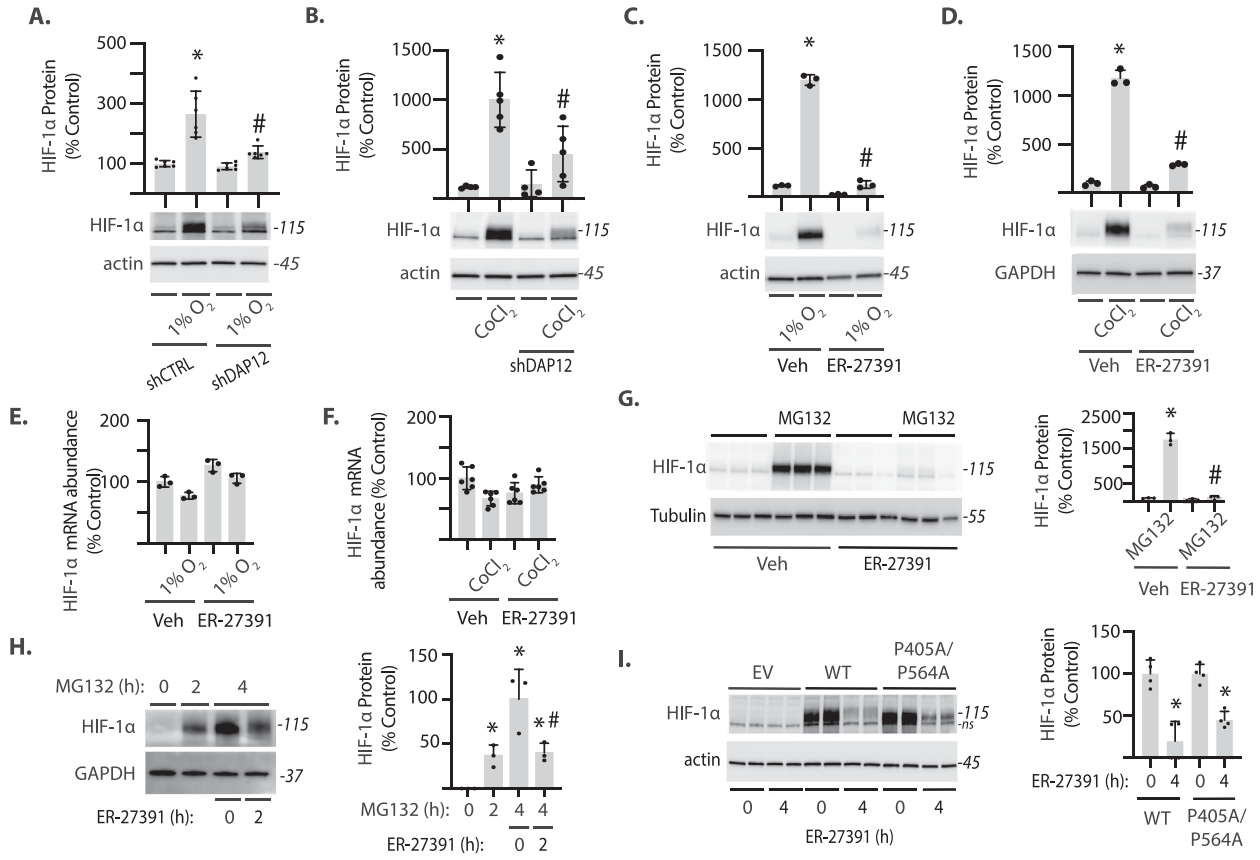

Figure 5. SYK facilitated HIF1α accumulation in Müller cells. (**A**) DAP12 expression was knocked down in MIO-M1 Müller cells by stable expression of shRNA (shDAP12). Control cells expressed a control shRNA (shCTRL). Cells were exposed to 1% oxygen for 24 hours and HIF1α expression was evaluated by Western blotting. Representative blots are shown. Protein molecular mass in kDa is indicated at *right* of blots. (**B**) MIO-M1 cells were exposed to medium supplemented with $CoCl_2$ for 4 hours. (**C–G**) MIO-M1 cells were treated with the SYK inhibtor ER-27391 or a vehicle (Veh) control and subsequently exposed to 1% oxygen (**C**, **E**), $CoCl_2$ (**D**, **F**), or the proteasome inhibitor MG132 (**G**) for 4 hours. (**E**, **F**) HIF1α mRNA abundance was determined by RT-PCR. (**H**) MIO-M1 cells were exposed to culture medium supplemented with MG132 for up to 4 hours. ER-27391 was added to culture medium after 2 hours of exposure to MG132 as indicated. (**I**) HEK293 cells were transfected to express empty vector (EV), wild-type HIF1α (WT), or HIF1α P405A/P564A. Cells were exposed to ER-27391 for up to 4 hours and HIF1α expression was determined by Western blotting. Values are means ± SD. $^*P < 0.05$ versus no treatment. $^\#P < 0.05$ versus no shDAP12 or vehicle.

DFO (Supplementary Fig. S3E). The suppressive effect of SYK inhibition on HIF1α induction was independent of a change in HIF1α mRNA abundance (Figs. 5E, 5F). Moreover, proteasomal inhibition was not sufficient to prevent the suppressive effect of ER-27391 on HIF1α accumulation (Figs. 5G, 5H). Indeed, ER-27391 suppressed expression of both wild-type HIF1α and a P405A/P564A variant that is deficient for proline hydroxylation (Fig. 5I). The results support that SYK inhibition suppresses expression of HIF1α by a posttranscriptional mechanism that does not require the proteasome or HIF1α hydroxylation at P405/P564.

SYK Inhibition Prevented Hypoxia-Induced Proangiogenic Cytokine Expression

VEGFA and angiopoietin-like 4 (ANGPTL4) are increased in the eyes of patients with diabetic macular edema and act synergistically to drive retinal permeability.[24] In MIO-M1 cells exposed to hypoxic conditions, mRNA abundance of VEGFA (Fig. 6A) and ANGPTL4 (Fig. 6B) was increased. DAP12 knockdown attenuated hypoxia-induced expression of both VEGFA and ANGPTL4 mRNAs. A similar suppressive effect was observed with SYK inhibition, as hypoxia-induced expression of VEGFA and ANGPTL4 was absent in cells treated with ER-27391 (Figs. 6C, 6D). $CoCl_2$ also promoted VEGFA and ANGPTL4 mRNA expression in MIO-M1 cells, and DAP12 knockdown reduced the effect (Supplementary Figs. S3F, S3G). Similarly, SYK inhibition with either ER-27391 (Figs. 6E, 6F) or R778 (Figs. 6G, 6H) attenuated $CoCl_2$-induced VEGFA and ANGPTL4 mRNA expression. In addition to secreting proangiogenic factors, Müller glia have also been implicated in the production of proinflammatory cytokines that contribute to DR progression.[4] To determine if SYK inhibition had a similar effect on inflammatory cytokine expression, TNFα, IL-1β, and IL6 expression were evaluated in MIO-M1 cells exposed to $CoCl_2$ (Supplementary Figs. S4A–C). Consistent with the suppressive effect on VEGFA and ANGPTL4, SYK inhibition reduced the expression of TNFα, IL-1β, and IL6 in cells exposed to $CoCl_2$ (Supplementary Figs. S4D–F).

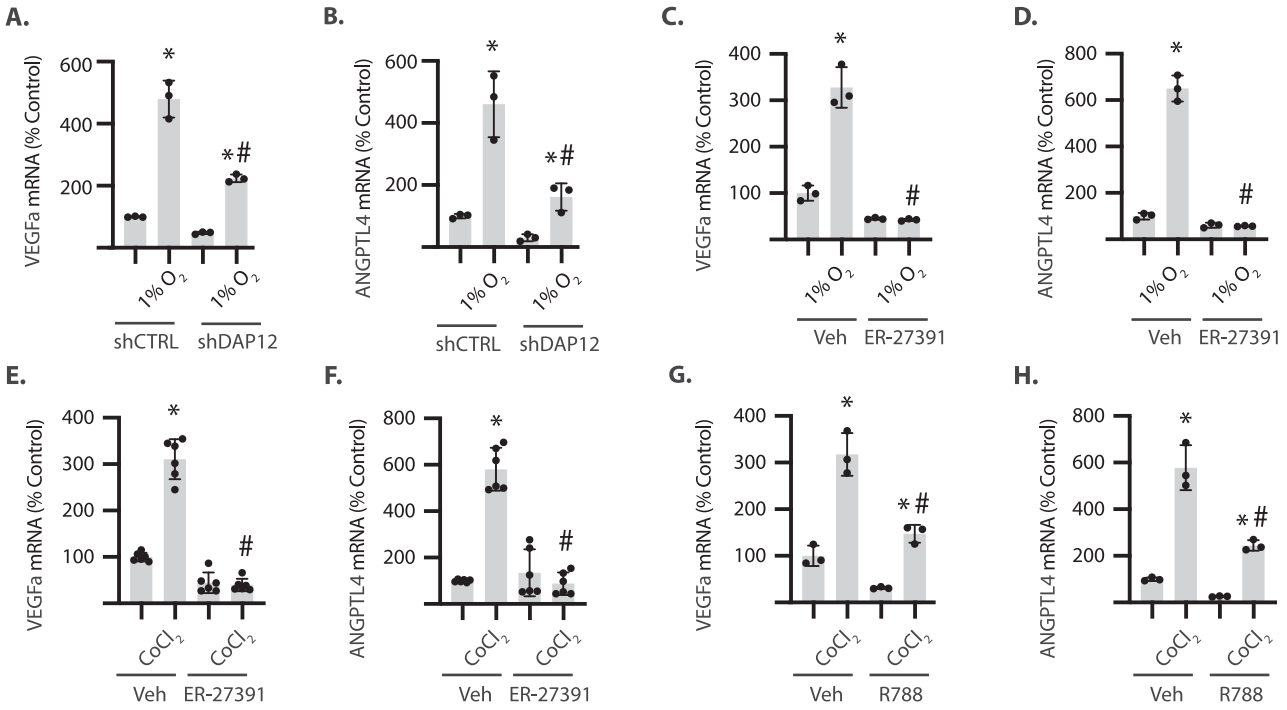

Figure 6. SYK contributed to pro-angiogenic cytokine expression in Müller cells. (**A**, **B**) DAP12 expression was knocked down in MIO-M1 Müller cells by stable expression of shRNA (shDAP12) or a control shRNA (shCTRL). Cells were exposed to 1% oxygen for 4 hours as indicated. (**C–F**) MIO-M1 cells were treated with the SYK inhibtor ER-27391 or a vehicle (Veh) control and subsequently exposed to 1% oxygen (**C**, **D**) or $CoCl_2$ (**E**, **F**) for 4 hours. (**G**, **H**) MIO-M1 cells were treated with the SYK inhibitor fostamatinib (R788) or a vehicle (Veh) control and subsequently exposed to $CoCl_2$ for 4 hours. Expression of mRNAs encoding VEGFA (**A**, **C**, **E**, **G**) and ANGPTL4 (**B**, **D**, **F**, **H**) was evaluated by RT-PCR. Values are means ± SD. *$P < 0.05$ versus no hypoxia or $CoCl_2$. #$P < 0.05$ versus shCTRL or vehicle.

Discussion

Retinal Müller glia provide critical homeostatic and trophic support to maintain both activity of retinal neurons and integrity of the blood–retinal barrier. Müller cells recycle neurotransmitters to prevent excitotoxicity, regulate metabolite levels, reabsorb fluid to prevent edema, and even contribute to the visual cycle.[3] In response to diabetes, Müller glia are known to produce a range of angiogenic and inflammatory cytokines that contribute to development of DR. The present study used *Pdgfra*-cre RiboTag mice to compare the impact of STZ-induced diabetes and HFHS diet on ribosome association of mRNAs in Müller glia. Association of mRNAs encoding TREM2, DAP12, and CSF1R with ribosomes isolated from Müller glia was upregulated in both models. Overall, the findings support a model wherein the TREM2/DAP12 receptor-adaptor complex signals via SYK to promote HIF1α stabilization and increased proangiogenic cytokine production by Müller glia (Supplementary Fig. S5).

Prior investigations focused on Müller glial gene expression and more recent retina-wide single-cell sequencing have used techniques such as microarray and RNA sequencing to identify "steady-state" differences in mRNA abundance. However, mRNA abundances are a relatively poor correlate for protein expression, and some studies suggest that variation in mRNA accounts for only ~40% of the global variation in protein abundance.[25,26] Translational control facilitates the selective recruitment of ribosomes to specific mRNAs to provide a rapid and reversible change in expression of specific proteins. Notably, mRNAs sensitive to translational control are most enriched in the gene categories of angiogenesis, synaptic transmission, and cell adhesion,[27] which are all key processes disrupted in the retina by diabetes. To investigate gene expression changes in Müller glia that were associated with early diabetes, sequencing analysis was performed on ribosome-associated mRNAs from the retina of RiboTag mice. Whereas there was no change in the abundance of mRNAs encoding TREM2, DAP12, and CSF1R in whole retina, association of these mRNAs with Müller glial ribosomes was enhanced by STZ diabetes or HFHS diet.

RiboTag mice express a fully functional HA-tagged ribosome in cells with Cre recombinase activity, allowing cell-specific isolation of translationally active mRNAs from heterologous tissues such as the retina. We previously demonstrated that RNA isolated from the retina of *Pdgfra*-cre;RiboTag mice was enriched for Müller cell markers.[17] An important limitation of this analysis is that in addition to Müller glia, other retinal glia may also exhibit recombinase activity. In particular, PDGFRa has been previously reported in astrocytes of the developing retina.[28] However, *Pdgfra*-cre recombinase-dependent nuclear lacZ expression in adult murine retina is exclusively localized to the inner nuclear layer.[21] Müller glial cell bodies localize to the inner nuclear layer, whereas the cell bodies of astrocytes are more commonly found in the retinal nerve fiber layer.[3] Consistent with Müller cell specificity in adult murine retina, $Rpl22^{HA}$ expression was observed in radially oriented processes that strongly colocalized with the Müller glia-specific marker GS.

TREM2 and DAP12 form a receptor-adaptor complex that is associated with neurodegenerative diseases, including Alzheimer and Parkinson diseases.[12] TREM2/DAP12

Investigative Ophthalmology & Visual Science

signaling has been principally explored in the context of microglia activation, where it promotes proliferation, migration, and phagocytosis of apoptotic neurons.[12] To our knowledge, a role for TREM2/DAP12 in retinal Müller glia has not been previously explored. The TREM2 immunoglobulin domain binds an array of ligands associated with tissue damage, including pathogen- and damage-associated molecular pattern molecules (i.e., pathogen-associated molecular patterns (PAMPs) and damage-associated molecular patterns (DAMPs)). Upon ligand binding by TREM2, tyrosine residues within the immunoreceptor tyrosine-based activation motif of DAP12 are phosphorylated, resulting in SYK recruitment and activation. SYK activation loop autophosphorylation is a key marker of SYK tyrosine kinase activity.[23] SYK autophosphorylation was enhanced in the retina of diabetic mice. In support of TREM2/DAP12 signaling to activate SYK in Müller cells, hypoxia-induced SYK autophosphorylation in MIO-M1 cells was prevented by DAP12 knockdown.

Oral administration of the SYK inhibitor R406 to STZ diabetic rats was previously found to reduce diabetes-induced retinal VEGF expression.[14] In coordination with reducing VEGF levels in the retina of STZ diabetic rats, SYK inhibition reduces retinal vascular permeability, prevents the appearance of acellular capillaries, and restores expression of tight junction proteins.[14] An important caveat to these benefits is that systemic delivery of R406 reduced fasting blood glucose concentrations in STZ diabetic rats; thus, it was unclear if the protective effects on DR pathology were achieved through SYK inhibition in specific retinal cells or secondary to improved glucose homeostasis. More recently, conditional SYK deletion in microglia was found to reduce microglial activation and proinflammatory cytokine expression in the retina of STZ diabetic mice.[29] In that study, SYK knockout in microglia prevented enhanced SYK expression in the retina of STZ diabetic mice; however, the majority of retinal SYK expression remained after tamoxifen-induced deletion, suggesting a role for the kinase in other retinal cell types. The proof-of-concept studies here provide evidence for upregulation of TREM2/DAP12 signaling in Müller cells to promote activation of SYK, stabilization of HIF1α, and enhanced proangiogenic cytokine expression.

SYK deletion was recently shown to reduce HIF1α expression in macrophages under hypoxic conditions,[15] and a similar suppressive effect on hypoxia-induced HIF1α was observed in splenocytes with the SYK inhibitor BAY 61-3606.[16] In Müller cells, SYK inhibition or DAP12 knockdown suppressed hypoxia-induced HIF1α expression. Studies here extend on the prior work by demonstrating that SYK inhibition did not alter HIF1α mRNA expression, nor was proteasomal activity required for the suppressive effect of SYK inhibition on HIF1α protein. Our findings are consistent with SYK acting via a proteasome-independent posttranscriptional mechanism to promote HIF1α protein content. A similar suppressive effect on ischemia-induced HIF1α expression in the retina was previously reported with the cardiac glycoside digoxin.[30] Digoxin prevents HIF1α mRNA translation, as it is unable to reduce HIF1α protein expression driven by an exogenous plasmid.[31] In contrast, SYK inhibition with ER-27391 attenuated the expression of both wild-type HIF1α and a hydroxylation-deficient P405A/P564A variant following plasmid transfection. Notably, these plasmids include the HIF1α mRNA coding sequence but lack the 5′ and 3′-UTR sequence elements that are required for digoxin to suppress HIF1α synthesis. Thus, digoxin and SYK inhibition likely act through different mechanisms to reduce HIF1α expression. While less well explored than proteasomal degradation, chaperone-mediated autophagy (CMA) is also a major regulator of HIF1α expression.[32] CMA mediates lysosomal degradation of specific KFERQ-like motif-bearing proteins in response to changes in the cellular environment.[33] Thus, one possibility is that SYK acts to prevent HIF1α degradation via CMA.

HIF1α protein expression is enhanced in the retina of STZ diabetic mice, and HIF1α deletion specifically in Müller glia is sufficient to prevent the increase.[34] The observation supports that diabetes specifically promotes HIF1α expression in Müller cells and is consistent with localization of HIF1α protein to Müller glia in the retina of diabetic patients.[9] Importantly, HIF1α deletion in Müller cells attenuates retinal vascular leakage and prevents increased VEGF production with diabetes.[34] Evidence also supports that Müller glia-derived VEGF is a key contributor to retinal vascular pathology in preclinical diabetes models.[5] Together, the prior studies support a key role for HIF1-dependent VEGF expression in the development of the vascular pathology that defines DR. Antibodies that block VEGF signaling have dramatically improved treatment outcomes in patients with DR.[35] However, VEGF is a relatively poor correlate with the extent of retinal edema,[36] implying that it likely acts in coordination with multiple other growth factors and cytokines to drive pathologic neovascularization. Indeed, Müller glia also upregulate production of ANGPTL4 to promote retinal vascular permeability.[9,24] The findings of this study support a role for diabetes-induced upregulation of TREM2/DAP12 signaling in Müller glia that acts via SYK to promote HIF1α stabilization and increased production of VEGF and ANGPTL4. Thus, local retinal SYK inhibition may represent a therapeutic step forward by not only suppressing VEGF mRNA transcription but also targeting the production of other critical factors that influence vascular permeability in both type 1 and type 2 diabetes.

Acknowledgments

The authors thank Dr. Alistair Barber (Penn State College of Medicine) for critically evaluating the manuscript.

Supported by National Institutes of Health grants R01 EY029702 and R01 EY032879 (to MDD).

Disclosure: **E.I. Yerlikaya,** None; **A.L. Toro,** None; **S. Sunilkumar,** None; **A.M. VanCleave,** None; **M. Leung,** None; **Y.I. Kawasawa**, None; **S.R. Kimball,** None; **M.D. Dennis,** None

References

1. Hammer SS, Busik JV. The role of dyslipidemia in diabetic retinopathy. *Vision Res*. 2017;139:228–236.
2. Antonetti DA, Barber AJ, Bronson SK, et al. Diabetic retinopathy: seeing beyond glucose-induced microvascular disease. *Diabetes*. 2006;55:2401–2411.
3. Reichenbach A, Bringmann A. Glia of the human retina. *Glia*. 2020;68:768–796.
4. Coughlin BA, Feenstra DJ, Mohr S. Müller cells and diabetic retinopathy. *Vision Res*. 2017;139:93–100.
5. Wang J, Xu X, Elliott MH, Zhu M, Le YZ. Müller cell-derived VEGF is essential for diabetes-induced retinal inflammation and vascular leakage. *Diabetes*. 2010;59:2297–2305.
6. Forsythe JA, Jiang BH, Iyer NV, et al. Activation of vascular endothelial growth factor gene transcription by hypoxia-inducible factor 1. *Mol Cell Biol*. 1996;16:4604–4613.

7. Semenza GL. Hypoxia-inducible factor 1: master regulator of O2 homeostasis. *Curr Opin Genet Dev*. 1998;8:588–594.
8. Cowan CS, Renner M, De Gennaro M, et al. Cell types of the human retina and its organoids at single-cell resolution. *Cell*. 2020;182:1623–1640.e1634.
9. Xin X, Rodrigues M, Umapathi M, et al. Hypoxic retinal Müller cells promote vascular permeability by HIF-1-dependent up-regulation of angiopoietin-like 4. *Proc Natl Acad Sci USA*. 2013;110:E3425–3434.
10. Asare-Bediako B, Noothi SK, Li Calzi S, et al. Characterizing the retinal phenotype in the high-fat diet and Western diet mouse models of prediabetes. *Cells*. 2020;9:464.
11. Lai AK, Lo AC. Animal models of diabetic retinopathy: summary and comparison. *J Diabetes Res*. 2013;2013:106594.
12. Konishi H, Kiyama H. Microglial TREM2/DAP12 signaling: a double-edged sword in neural diseases. *Front Cell Neurosci*. 2018;12:206.
13. Zou W, Reeve JL, Liu Y, Teitelbaum SL, Ross FP. DAP12 couples c-Fms activation to the osteoclast cytoskeleton by recruitment of Syk. *Mol Cell*. 2008;31:422–431.
14. Su X, Sun ZH, Ren Q, et al. The effect of spleen tyrosine kinase inhibitor R406 on diabetic retinopathy in experimental diabetic rats. *Int Ophthalmol*. 2020;40:2371–2383.
15. Joshi S, Liu KX, Zulcic M, et al. Macrophage Syk-PI3Kγ inhibits antitumor immunity: SRX3207, a novel dual Syk-PI3K inhibitory chemotype relieves tumor immunosuppression. *Mol Cancer Ther*. 2020;19:755–764.
16. Jang JW, Park S, Moon EY. Spleen tyrosine kinase regulates crosstalk of hypoxia-inducible factor-1α and nuclear factor (erythroid-derived2)-like 2 for B cell survival. *Int Immunopharmacol*. 2021;95:107509.
17. Dierschke SK, Toro AL, Miller WP, Sunilkumar S, Dennis MD. Diabetes enhances translation of Cd40 mRNA in murine retinal Müller glia via a 4E-BP1/2-dependent mechanism. *J Biol Chem*. 2020;295:10831–10841.
18. Miller WP, Toro AL, Sunilkumar S, et al. Müller glial expression of REDD1 is required for retinal neurodegeneration and visual dysfunction in diabetic mice. *Diabetes*. 2022;71:1051–1062.
19. Miller WP, Sunilkumar S, Giordano JF, Toro AL, Barber AJ, Dennis MD. The stress response protein REDD1 promotes diabetes-induced oxidative stress in the retina by Keap1-independent Nrf2 degradation. *J Biol Chem*. 2020;295:7350–7361.
20. Sanz E, Yang L, Su T, Morris DR, McKnight GS, Amieux PS. Cell-type-specific isolation of ribosome-associated mRNA from complex tissues. *Proc Natl Acad Sci USA*. 2009;106:13939–13944.
21. Roesch K, Jadhav AP, Trimarchi JM, et al. The transcriptome of retinal Müller glial cells. *J Comp Neurol*. 2008;509:225–238.
22. Otero K, Turnbull IR, Poliani PL, et al. Macrophage colony-stimulating factor induces the proliferation and survival of macrophages via a pathway involving DAP12 and beta-catenin. *Nat Immunol*. 2009;10:734–743.
23. Zhang J, Billingsley ML, Kincaid RL, Siraganian RP. Phosphorylation of Syk activation loop tyrosines is essential for Syk function: an in vivo study using a specific anti-Syk activation loop phosphotyrosine antibody. *J Biol Chem*. 2000;275:35442–35447.
24. Sodhi A, Ma T, Menon D, et al. Angiopoietin-like 4 binds neuropilins and cooperates with VEGF to induce diabetic macular edema. *J Clin Invest*. 2019;129:4593–4608.
25. Schwanhäusser B, Busse D, Li N, et al. Global quantification of mammalian gene expression control. *Nature*. 2011;473:337–342.
26. Jovanovic M, Rooney MS, Mertins P, et al. Immunogenetics: dynamic profiling of the protein life cycle in response to pathogens. *Science*. 2015;347:1259038.
27. Wellensiek BP, Larsen AC, Stephens B, et al. Genome-wide profiling of human cap-independent translation-enhancing elements. *Nat Methods*. 2013;10:747–750.
28. Fruttiger M, Calver AR, Krüger WH, et al. PDGF mediates a neuron-astrocyte interaction in the developing retina. *Neuron*. 1996;17:1117–1131.
29. Liu X, Xu B, Gao S. Spleen tyrosine kinase mediates microglial activation in mice with diabetic retinopathy. *Transl Vis Sci Technol*. 2021;10:20.
30. Yoshida T, Zhang H, Iwase T, Shen J, Semenza GL, Campochiaro PA. Digoxin inhibits retinal ischemia-induced HIF-1alpha expression and ocular neovascularization. *FASEB J*. 2010;24:1759–1767.
31. Zhang H, Qian DZ, Tan YS, et al. Digoxin and other cardiac glycosides inhibit HIF-1alpha synthesis and block tumor growth. *Proc Natl Acad Sci USA*. 2008;105:19579–19586.
32. Hubbi ME, Hu H, Kshitiz Ahmed I, Levchenko A, Semenza GL. Chaperone-mediated autophagy targets hypoxia-inducible factor-1α (HIF-1α) for lysosomal degradation. *J Biol Chem*. 2013;288:10703–10714.
33. Kirchner P, Bourdenx M, Madrigal-Matute J, et al. Proteome-wide analysis of chaperone-mediated autophagy targeting motifs. *PLoS Biol*. 2019;17:e3000301.
34. Lin M, Chen Y, Jin J, et al. Ischaemia-induced retinal neovascularisation and diabetic retinopathy in mice with conditional knockout of hypoxia-inducible factor-1 in retinal Müller cells. *Diabetologia*. 2011;54:1554–1566.
35. Gross JG, Glassman AR, Jampol LM, et al. Panretinal photocoagulation vs intravitreous ranibizumab for proliferative diabetic retinopathy: a randomized clinical trial. *JAMA*. 2015;314:2137–2146.
36. Kita T, Clermont AC, Murugesan N, et al. Plasma kallikrein-kinin system as a VEGF-independent mediator of diabetic macular edema. *Diabetes*. 2015;64:3588–3599.

Investigative Ophthalmology & Visual Science